

## Magnetotunneling analysis of the scattering processes in a double-barrier structure with a two-dimensional emitter

Y. Galvao Gobato

*Laboratoire de Physique de la Matière Condensée, Département de Physique de l'Ecole Normale Supérieure,  
24 rue Lhomond, 75005 Paris, France*

F. Chevoir

*Thomson-CSF, Laboratoire Central de Recherches, Domaine de Corbeville, Boîte Postale 10, 91401 Orsay, France*

J. M. Berroir

*Laboratoire de Physique de la Matière Condensée, Département de Physique de l'Ecole Normale Supérieure,  
24 rue Lhomond, 75005 Paris, France*

P. Bois

*Thomson-CSF, Laboratoire Central de Recherches, Domaine de Corbeville, Boîte Postale 10, 91401 Orsay, France*

Y. Guldner

*Laboratoire de Physique de la Matière Condensée, Département de Physique de l'Ecole Normale Supérieure,  
24 rue Lhomond, 75005 Paris, France*

J. Nagle

*Thomson-CSF, Laboratoire Central de Recherches, Domaine de Corbeville, Boîte Postale 10, 91401 Orsay, France*

J. P. Vieren

*Laboratoire de Physique de la Matière Condensée, Département de Physique de l'Ecole Normale Supérieure,  
24 rue Lhomond, 75005 Paris, France*

B. Vinter

*Thomson-CSF, Laboratoire Central de Recherches, Domaine de Corbeville, Boîte Postale 10, 91401 Orsay, France*

(Received 16 July 1990; revised manuscript received 12 September 1990)

We report magnetotunneling results obtained in a high-quality GaAs-Al<sub>x</sub>Ga<sub>1-x</sub>As double-barrier diode with large undoped spacers. Magneto-oscillations of the current in the resonance situation show the two-dimensionality of the source electrons resulting from the formation of an accumulation layer in the emitter. In the off-resonance regime, three different sets of current oscillations have been observed, which correspond to tunneling with elastic- or inelastic-scattering processes on the one hand and to the charge modulation of the accumulation layer on the other hand. From these data the energies of the quantized level in the accumulation layer and in the well are determined as a function of the voltage, in very good agreement with theoretical calculations. Finally, we present theoretical simulations of scattering-assisted magnetotunneling, which account for the experimental data.

Recently there has been great interest in magnetotunneling studies of GaAs-Al<sub>x</sub>Ga<sub>1-x</sub>As double-barrier diodes. In the resonant regime, when a magnetic field  $B$  is applied parallel to the current  $I$ , oscillations have been reported in the  $I(B)$  curves,<sup>1-4</sup> from which the charge buildup in the well and the dimensionality (2D or 3D) of the emitter can be deduced. Theoretical models for this regime have been published:<sup>5-8</sup> the effect of scattering processes on the resonant transmission has been studied by Schulz and Tejedor,<sup>6</sup> by means of the Stone and Lee phenomenological model.<sup>9</sup> But it is also necessary to include the broadening of the Landau levels.<sup>8</sup> However, the effect of scattering processes on the current becomes

even more important in the off-resonant regime, as evidenced by magnetotunneling analysis of the valley current;<sup>10-13</sup> then magneto-oscillations arise from elastic and inelastic tunneling processes with no conservation of the transverse momentum. For instance, electrons can tunnel from a Landau level of the emitter into a Landau level of the quantum well with a different index, the total energy of this incoherent process being conserved. Inelastic processes with LO-phonon emission and conserving or nonconserving Landau-level index were also observed.

We report here new magnetotunneling results obtained in a GaAs-Al<sub>x</sub>Ga<sub>1-x</sub>As double-barrier diode with a

two-dimensional accumulation layer at the emitter side, together with calculations of scattering-assisted magnetotunneling in this device, including intrinsic processes [acoustic and longitudinal optical (LO) phonons, alloy disorder] and interface roughness and taking into account the broadening of the Landau levels. Strong magneto-oscillations of the current are observed both in the resonance and in the off-resonance regimes. The magnetic field versus voltage diagram of the maxima of these oscillations clearly shows three sets of lines, each converging to a different voltage at zero magnetic field. The first two sets correspond to tunneling with elastic- and inelastic-scattering processes. The third set corresponds to valley current oscillations occurring when a Landau level of the 2D emitter crosses the emitter Fermi level. Such oscillations are in fact very similar to those observed in the case of a single-barrier diode.<sup>14</sup> From these three sets of curves, one can deduce the energies of the quantized level in the accumulation layer ( $E_{acc}$ ) and in the well ( $E_w$ ) relative to the emitter Fermi energy  $E_f$  as a function of the voltage  $V$ , while in the previously reported experiments, only the  $E_{acc}$ - $E_w$  separation could be measured.<sup>12</sup> These measurements are shown to be in very good agreement with self-consistent calculations of the device band structure and of the quantized level energies. Moreover, we show that our theory of scattering-assisted tunneling<sup>15</sup> may easily be extended to describe the magnetotransport in the off-resonant regime. This first quantitative treatment of scattering-assisted magnetotunneling is in good agreement with experimental results.

Our symmetric-double-barrier structure was grown by molecular-beam epitaxy on an  $n^+$ -type GaAs substrate. Both emitter and collector consisted of  $0.3 \mu\text{m}$  of GaAs, Si doped to  $10^{18} \text{cm}^{-3}$  and of a large spacer layer ( $600 \text{ \AA}$ ) of nonintentionally doped GaAs. The barriers are  $100\text{-\AA}$ -thick  $\text{Al}_{0.31}\text{Ga}_{0.69}\text{As}$  layers and the well is a  $50\text{-\AA}$  nonintentionally doped GaAs layer. The results we report here have been obtained on a  $60 \times 60\text{-}\mu\text{m}^2$  device defined by standard mesa etching techniques. The voltage is measured with the use of a pseudo-four-terminal technique.

The zero-magnetic-field  $I(V)$  characteristics of our structure at  $T=4.2 \text{ K}$  is shown in Fig. 1(a). The peak to valley current ratio is about 12, the maximum current density is  $12.2 \text{ A cm}^{-2}$ , and a very-well-separated phonon-assisted tunneling feature<sup>2</sup> is observed after the resonance voltage. Figure 2 shows the calculated band structure of the device at resonance obtained by solving the Poisson equation in the Thomas-Fermi approximation in both contacts and assuming a constant Fermi level in the whole emitter. Due to the doping profile, an electrostatic bump forms between the emitter contact and the emitter barrier, and a quantized level  $E_{acc}$  appears in the accumulation layer corresponding to a peaked transmission through the structure. The resonant tunneling process involves anticrossing of the two quantized levels  $E_{acc}$  and  $E_w$ , which explains the narrowness of the resonance. The existence of a well-resolved phonon structure is another consequence of the injection from a 2D emitter: the effective Fermi energy  $E_f - E_{acc}$  remains smaller than the LO-phonon energy, so that the LO-phonon emission

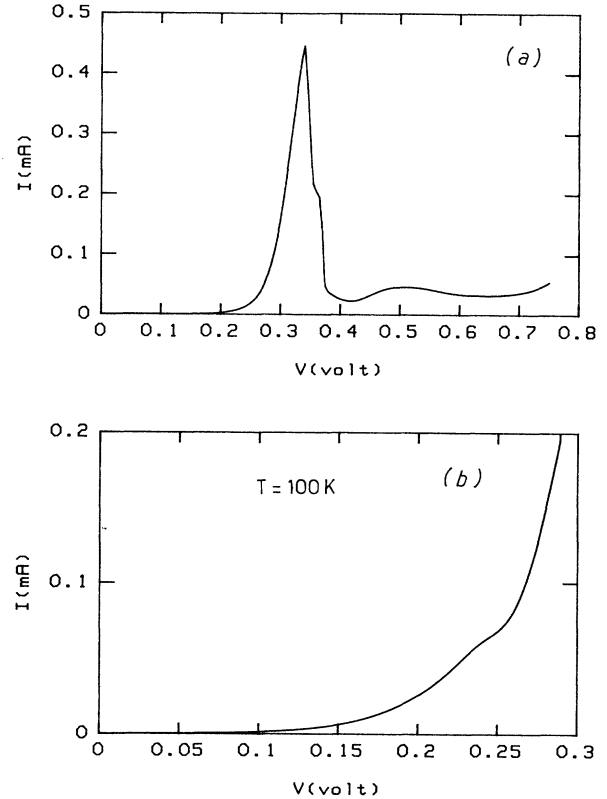


FIG. 1. (a) Current-voltage characteristics of the device at  $4.2 \text{ K}$ . The peak current density is  $12.2 \text{ A cm}^{-2}$ . (b) Detail of the  $I(V)$  characteristics at  $100 \text{ K}$  showing the contribution of ballistic electrons (around  $0.25 \text{ V}$ ).

begins well after the resonance regime, similarly to the case of a weakly doped 3D emitter.<sup>15</sup> Using the potential profile, we simulate the  $I(V)$  characteristics at  $4 \text{ K}$  (Fig. 3). In the resonance regime we calculate the coherent tunneling current. The small feature before the narrow resonance peak is due to the contribution of ballistic elec-

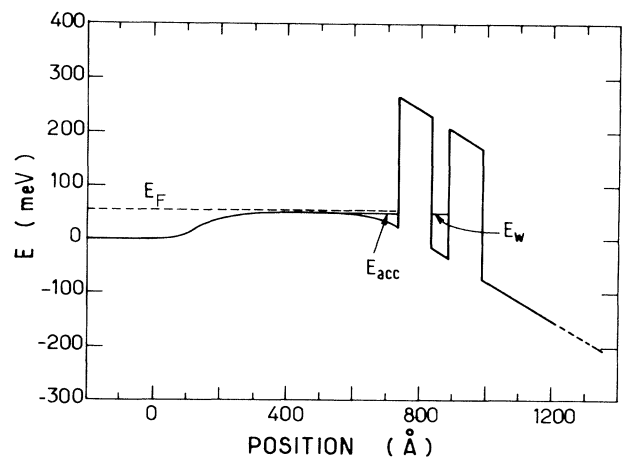


FIG. 2. Calculated band structure at the resonance voltage. The dashed line indicates the emitter Fermi level. A doping level of  $10^{16} \text{ cm}^{-3}$  was assumed in the spacers.

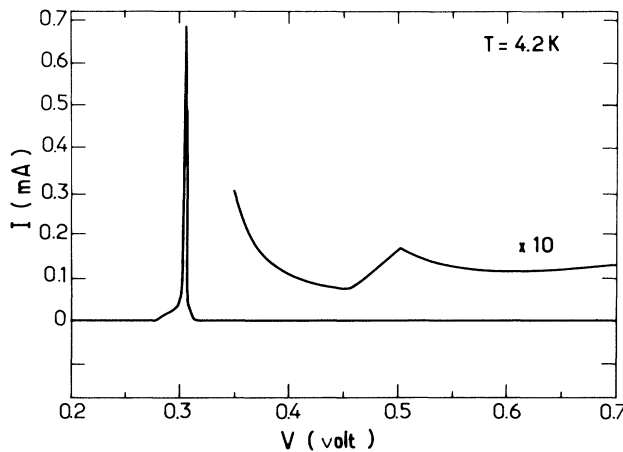


FIG. 3. Calculated current-voltage characteristics of the device at 4.2 K. The peak current density is  $19.4 \text{ A cm}^{-2}$ .

trons over the bump: this is the 3D part of the resonant current.<sup>8</sup> In the off-resonance regime we have previously proposed<sup>15</sup> to treat the valley current as a capture process from the emitter into the well. We have checked that the contribution of ballistic electrons is very small and that the 2D emitter level is strongly supplied by tunneling through the bump, from which we conclude that, in the off-resonance regime, the transport mechanism is dominated by scattering-assisted tunneling between the two 2D levels. These scattering currents are calculated by using Fermi's golden rule between the unperturbed states of the tunneling structure:<sup>15,16</sup> this calculation involves the envelope wave functions in the 1D potential shown in Fig. 2, and takes into account the transfer of momentum in the layers, so that it is truly 3D. We have taken into account the contribution of intrinsic scattering processes (LO phonons, acoustic phonons, alloy disorder) and of interface roughness, which seems to be the major scattering source near the resonance peak.<sup>17</sup> In these calculations the only free parameter is the interface roughness correlation length for which we take a value of  $65 \text{ \AA}$ .<sup>18</sup> The voltages of both resonant and phonon-assisted current peaks are in good agreement with those experimentally observed [Fig. 1(a)] and the orders of magnitude of the two current peaks are well described by the theory. The contribution of ballistic electrons is observed in the rise of the resonance peak ( $V=0.25 \text{ V}$ ) in the  $I(V)$  characteristics at 100 K [Fig. 1(b)]. It is important to point out that this feature is not due to phonon-absorption-assisted tunneling since no important variation is observed with further temperature increase and since such a phonon-absorption feature would occur at a much lower voltage.

We have performed magnetotunneling experiments at 4.2 K with the magnetic field applied parallel to the current and varied between 0 and 12 T. A typical  $I(V)$  characteristic (at  $B=8.1 \text{ T}$ ) is shown in Fig. 4. These  $I(V)$  curves show no significant changes in the resonance regime, except for a slight increase of the resonant peak voltage  $V_p$ . But strong oscillations are observed in the

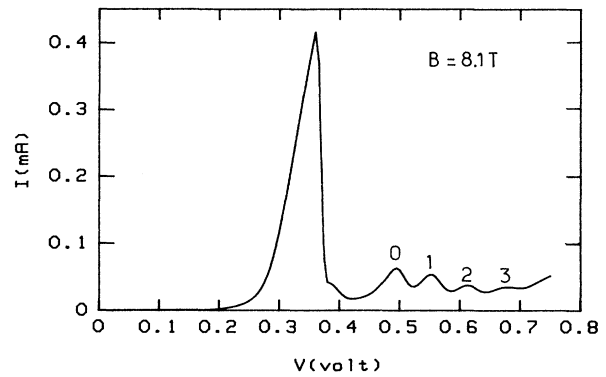


FIG. 4. Measured  $I(V)$  characteristics for  $B=8.1 \text{ T}$  at 4.2 K, showing the magneto-oscillations (denoted 0,1,2,3) in the valley current.

valley current: when increasing magnetic field, additional peaks (denoted 1,2,3,...) emerge from the zero-magnetic-field LO-phonon feature (denoted 0), whose amplitude is enhanced. In fact, the analysis of the magneto-oscillations of the current at fixed voltage [ $I(B)$  curves] appears more instructive: well-resolved oscillations are observed in the whole range of voltage. In the resonance regime, for which the typical  $I(B)$  curve is shown in Fig. 5(a) (at the onset of the resonance process), we recover the results previously described in Ref. 3 for similar double-barrier structures with thick undoped spacer layers: the oscillations are periodic in  $B^{-1}$  and the oscillation period presents a very small linear variation with the voltage. This variation cannot be explained in terms of 3D-2D resonant tunneling but is evidence of the 2D injection of electrons. The magnetooscillations arise from the variation of transmission and supply function due to the charge modulation of the mixed resonant state, during anticrossing of  $E_{acc}$  and  $E_w$ .

We now discuss the results obtained in the off-resonance regime ( $V > 0.33 \text{ V}$ ). Typical  $I(B)$  curves at 4.2 K are shown in Fig. 5(b) ( $V=0.61 \text{ V}$ ) and in Fig. 5(c) ( $V=0.71 \text{ V}$ ). Sharp and pronounced oscillations are observed in these  $I(B)$  curves which present more features than  $I(V)$  characteristics, in particular at low magnetic fields ( $B < 4 \text{ T}$ ). To determine the origin of these current oscillations,  $I(B)$  curves have been measured for various voltages from 0.33 to 0.8 V with an increment of 0.01 V. The data are summarized in Fig. 6, in a magnetic field versus voltage diagram where dots represent current maxima in the valley regime and triangles indicate the position of the resonant current peak. The data are very complex, but it is clear that the dots group themselves into three sets of straight lines, converging to  $V=0.33$ , 0.48, and  $-0.4 \text{ V}$ , respectively at zero magnetic field. Note that a similar fan chart is obtained when the positions of the current minima are plotted instead of those of the maxima.

The first set consists of two lines labeled 1' and 2' converging to the resonant peak voltage ( $V=0.33 \text{ V}$ ) and is explained as follows. When a longitudinal magnetic field

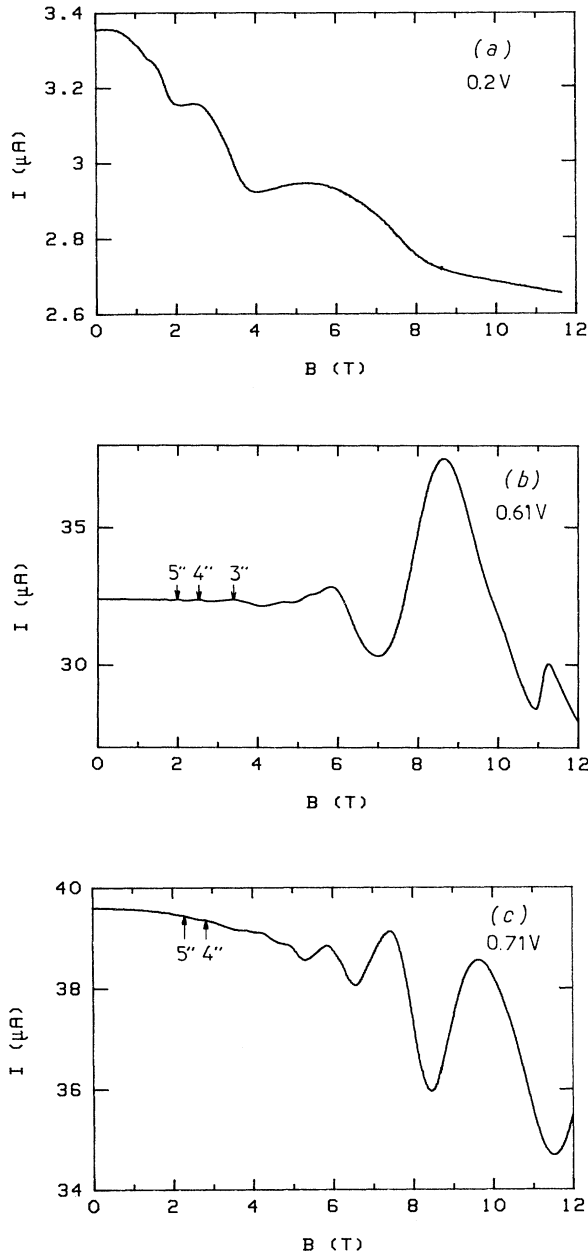


FIG. 5. Magneto-oscillations of the current for various voltages: (a)  $V=0.2$  V; (b)  $V=0.61$  V; (c)  $V=0.71$  V. The peaks corresponding to the third series of oscillations are labeled.

$B$  is applied, the transverse motion of 2D electrons in both accumulation layer and well is quantized into Landau orbits of energy  $(n + 1/2)\hbar\omega_c$ , where  $\hbar\omega_c$  is the GaAs cyclotron energy. Beyond the resonance voltage,  $E_{acc} > E_w$  and for voltages such that

$$E_{acc} - E_w = m\hbar\omega_c, \quad (1)$$

where  $m$  is an integer, electrons in the  $n$ th Landau level of the accumulation layer can tunnel by elastic scattering

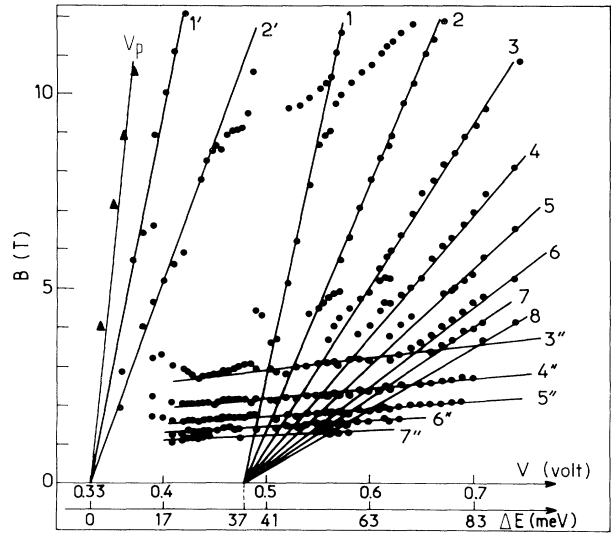


FIG. 6. Magnetic field vs voltage diagram of the current maxima (dots in the valley region and triangles for the resonant peak). Solid lines are the calculated  $B(V)$  dependence of the current maxima. The  $\Delta E$  scale is obtained as described in the text.

into the  $(n + m)$ th Landau level of the well, and a current maximum is observed.<sup>11</sup> Such transitions correspond to incoherent elastic tunneling processes because transverse kinetic energy and momentum must be transferred to the longitudinal direction via elastic scattering (alloy disorder, interface roughness or acoustic phonon scattering). The lines labeled 1' and 2' in Fig. 6 correspond to such an incoherent elastic tunneling process with  $m=1$  and 2 respectively.

The second set consists of eight lines converging to 0.48 V which is the voltage of the LO-phonon-related peak. These current maxima occur when the electron transfer between Landau levels is assisted by the emission of a LO phonon<sup>11</sup> (of energy  $\hbar\omega_{LO}$ ), when the following condition is satisfied:

$$E_{acc} - E_w = m\hbar\omega_c + \hbar\omega_{LO}. \quad (2)$$

As many as eight inelastic transitions with  $m=1, 2, \dots, 8$  are observed in our  $I(B)$  experiments. Only the first inelastic transitions are observed directly in  $I(V)$  characteristics under applied magnetic field. For instance, the peaks labeled 1, 2, 3 in Fig. 4 correspond to inelastic transitions with  $m=1, 2, 3$ .

Each of these two sets of curves gives separately the correspondence between the energy difference  $\Delta E = E_{acc} - E_w$  and the voltage. Note in Fig. 6, that several deviations from straight lines are observed around the crossing points of the three sets of lines, for instance, where both elastic- and inelastic-scattering processes are allowed. The  $\Delta E$  scale calculated from the linear part of the curves is shown in Fig. 6, where we have used  $\hbar\omega_{LO} = 37$  meV and  $\hbar\omega_c = 1.7$  B meV/T. The proportionality factor between  $\Delta E$  and  $e\Delta V$  is found to vary

slowly from 0.24 to 0.22 with increasing voltages. The  $B(V)$  dependences of the current maxima, as calculated from (1) and (2), are represented by the solid lines 1', 2' and 1, 2, . . . , 8 in Fig. 6. The agreement with experimental data is satisfactory.

Additional features are observed in the  $I(B)$  curves but not in the  $I(V)$  characteristics under magnetic field. The maxima of these oscillations are represented in Fig. 6 by the third set of curves labeled 3'', 4'', . . . , 7'' which extrapolate to negative voltage and is periodic in  $B^{-1}$ . In the off-resonance regime, coherent tunneling in our structure behaves as tunneling from a two-dimensional electron gas across a single barrier so that we believe that this third series of oscillations is very similar to the one reported by Böckenhoff *et al.*<sup>14</sup> in a single-barrier diode with an accumulation layer formed in the emitter under bias. These authors have calculated the magnetic-field dependence of the tunnel current and they have shown that, for a given voltage, variation of  $B$  slightly modifies the energy  $E_f - E_{acc}$  and therefore the electron density of the accumulation layer, but strongly modulates the tunnel current because of the exponential variation of the transmission with respect to electron energy. Current jumps occur for integer filling factors of the 2D electron gas which explains the  $B^{-1}$  periodicity of the oscillations. This  $B^{-1}$  periodicity presents a very low variation as a function of the voltage, as in the resonance regime. According to our interpretation of these oscillations, the  $B^{-1}$  periodicity gives the variation  $\Delta E_{acc}/\Delta V$ , which is found to be  $\approx 20$  meV/V in the voltage range from 0.4 to 0.7 V.

The crosses in Fig. 7 show the experimental dependence  $E_{acc}(V)$  determined from the third group of oscillations and  $E_w(V)$  deduced from our data, using the  $\Delta E(V)$  dependence derived from the two other groups of oscillations. The solid lines in Fig. 7 are the theoretical variations  $E_{acc}(V)$  and  $E_w(V)$  obtained by solving the Poisson equation self-consistently. The zero of energy is the

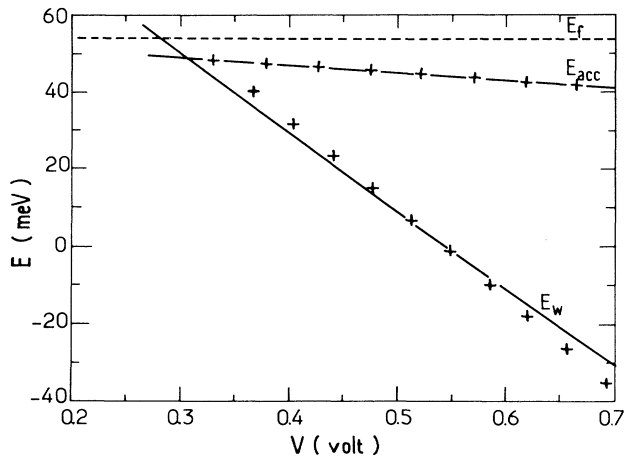


FIG. 7. Experimental (crosses) and theoretical (solid lines) variation with voltage of the quantized level energies ( $E_{acc}$  and  $E_w$ ), relative to the emitter Fermi energy (dashed line). The zero of energy is taken at the conduction-band edge in the emitter contact.

conduction-band edge at the emitter contact (see Fig. 2). The constant Fermi energy in the emitter ( $E_f = 54$  meV corresponding to a doping of  $10^{18}$  cm $^{-3}$ ) is represented by the dashed line in Fig. 7. The agreement between theory and experiment (solid lines and crosses) is excellent. Furthermore, one can also deduce the emitter Fermi level from the third group of oscillations, using the relation  $E_f - E_{acc} = \hbar e B_f / m^*$ , where  $B_f$  is the fundamental field defined from the periodicity of these oscillations and  $m^*$  is the GaAs conduction-band mass. An agreement within a few meV with the theoretical value of  $E_f$  is obtained, which is satisfactory if one considers the use of the Thomas-Fermi approximation in the model.<sup>19</sup>

Our theory of scattering-assisted tunneling may be easily extended to describe magnetotransport in the off-resonant regime. This provides a theoretical and quantitative treatment of the influence of a longitudinal magnetic field on the valley current. The application of a magnetic field perpendicular to the layer quantizes the transverse motion of electrons in Landau orbits. These levels are broadened by the various scattering mechanisms, essentially either in the accumulation layer or inside the well, depending on where the level is localized. The shape of the resulting density of states (DOS) has been investigated both experimentally and theoretically.<sup>20</sup> In our calculations we assume a Gaussian shape of Landau levels and use the following harmonic approximation of this DOS:

$$D(\epsilon_{\parallel}) = \frac{m^*}{2\pi\hbar^2} \left\{ 1 - 2 \exp \left[ - \left( \frac{\pi\Gamma}{\hbar\omega_c} \right)^2 \right] \cos \left[ \frac{2\pi\epsilon_{\parallel}}{\hbar\omega_c} \right] \right\}. \quad (3)$$

The 2D emitter provides electrons with the Fermi-Dirac statistics  $f_{FD}$  depending on their transverse energy  $\epsilon_{\parallel}$ . The valley current is dominated by the capture process of these electrons into the well:

$$J = 2e \int_0^{\infty} d\epsilon_{\parallel} D(\epsilon_{\parallel}) f_{FD}(\epsilon_{\parallel}) W(\epsilon_{\parallel}). \quad (4)$$

If the capture process is described by a perturbation  $H^p$ , then the capture rate is given by Fermi's golden rule:

$$W(\epsilon_{\parallel}) = \frac{8\pi^3 a_0^2}{h} |\langle \xi_{acc} n_{\epsilon_{\parallel}} | H^p | \xi_w n_w \rangle|^2 D(\epsilon_{\parallel w}). \quad (5)$$

$a_0$  is the cyclotron radius;  $\xi_{acc}$ ,  $\xi_w$  are the accumulation layer and well envelope wave functions; the transverse energy in the well  $\epsilon_{\parallel w}$  is deduced from energy conservation;  $n_{\epsilon_{\parallel}}$  and  $n_w$  are the corresponding Landau levels. In our simulation we take into account the same scattering processes as in the zero-magnetic-field case (acoustic and LO phonons, alloy disorder, and interface roughness) and we assume a broadening of Landau levels  $\Gamma = \sqrt{B}$  meV/ $\sqrt{T}$ . The detail of the calculation of the matrix elements of interaction may be found elsewhere.<sup>8,21</sup> We stress the fact that the resulting expression of the current involves the product of emitter and well DOS and therefore the valley current is very sensitive to the magnetic field. The calculated  $I(V)$  characteristics in the valley regime are shown in Fig. 8 for several magnetic fields. The order of magnitude and the shape of the magneto-oscillations corre-

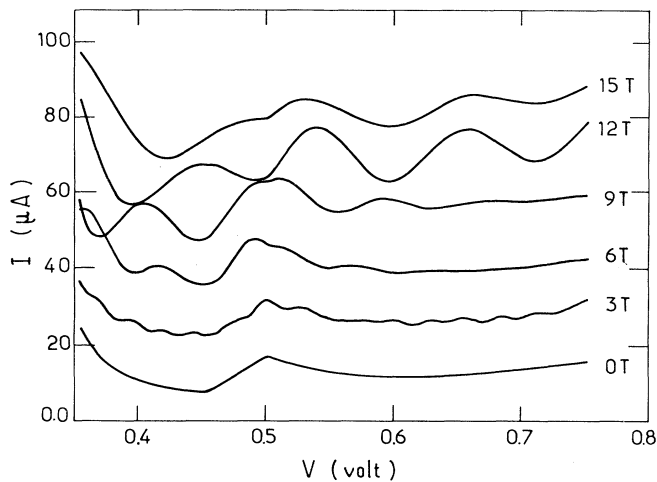


FIG. 8. Simulation of scattering-assisted magnetotunneling for several magnetic fields at  $T=4.2$  K. The scale is for the zero-magnetic-field curve. Each curve is shifted from the preceding one by  $14.4 \mu\text{A}$ .

sponding to both elastic and inelastic-scattering processes are in good agreement with the experimental observations (see Fig. 4).

In conclusion, we have performed magnetotunneling measurements in a high-quality double-barrier structure

with large undoped spacers. In the resonance regime, magneto-oscillations of the current show that the electron source is two-dimensional. In the valley regime, three different sets of magneto-oscillations of the current have been observed. They correspond to elastic- or inelastic-scattering-assisted tunneling on one hand, and to the magnetic-field modulation of the charge in the accumulation layer on the other hand. The analysis of these three sets of oscillations gives the energy of the quantized levels involved in the transport as a function of the voltage, as well as the emitter Fermi energy. These results are in very good agreement with a calculation of the band structure of the device and of the energies of the quantized levels. Finally, we have presented a simulation of scattering-assisted magnetotunneling in our device using a model which includes the contribution of intrinsic processes and of interface roughness and which takes into account the broadening of the Landau levels. These calculations account for the experimental  $I(V)$  characteristics under longitudinal magnetic field and should allow further investigation of inter-Landau-level scattering.

This work was supported by the Ministère de la Recherche et de la Technologie. Two of the authors would like to acknowledge financial support from Coordenação de Aperfeiçoamento de Pessoal de Nível Superior, Brazil (Y.G.G.), and from the Ecole Nationale des Ponts et Chaussées (F.C.).

- <sup>1</sup>E. E. Mendez, L. Esaki, and W. I. Wang, *Phys. Rev. B* **33**, 2893 (1986).
- <sup>2</sup>V. J. Goldman, D. C. Tsui, and J. E. Cunningham, *Phys. Rev. B* **35**, 9387 (1987).
- <sup>3</sup>D. Thomas, F. Chevoir, P. Bois, E. Barbier, Y. Guldner, and J. P. Vieren, *Superlatt. Microstruct.* **5**, 219 (1989).
- <sup>4</sup>A. Zaslavsky, D. C. Tsui, M. Santos, and M. Shayegan, *Phys. Rev. B* **40**, 9829 (1989).
- <sup>5</sup>C. E. T. Gonçalves da Silva and E. E. Mendez, *Phys. Rev. B* **38**, 3994 (1988).
- <sup>6</sup>P. A. Schulz and C. Tejedor, *Phys. Rev. B* **41**, 3053 (1990).
- <sup>7</sup>W. Pötz, *Phys. Rev. B* **41**, 12111 (1990).
- <sup>8</sup>F. Chevoir and B. Vinter, in *Resonant Tunneling: Physics and Applications*, edited by L. L. Chang (Plenum, New York, 1990).
- <sup>9</sup>A. D. Stone and P. A. Lee, *Phys. Rev. Lett.* **54**, 1196 (1985).
- <sup>10</sup>L. Eaves, G. A. Toombs, F. W. Sheard, C. A. Payling, M. L. Leadbeater, E. S. Alves, T. J. Foster, P. E. Simmonds, M. Henini, O. H. Hugues, J. C. Portal, G. Hill, and M. A. Pate, *Appl. Phys. Lett.* **52**, 212 (1988).
- <sup>11</sup>M. L. Leadbeater, E. S. Alves, L. Eaves, M. Henini, O. H.

- Hugues, A. Celeste, J. C. Portal, G. Hill, and M. A. Pate, *Phys. Rev. B* **39**, 3438 (1989).
- <sup>12</sup>C. H. Yang, M. J. Yang, and Y. C. Kao, *Phys. Rev. B* **40**, 6272 (1989).
- <sup>13</sup>J. J. L. Rascol, K. P. Martin, S. B. Amor, R. J. Higgins, A. Celeste, J. C. Portal, A. Torabi, H. M. Harris, and C. J. Summers, *Phys. Rev. B* **41**, 3733 (1990).
- <sup>14</sup>E. Böckenhoff, K. v. Klitzing and K. Ploog, *Phys. Rev. B* **38**, 10 120 (1988).
- <sup>15</sup>F. Chevoir and B. Vinter, *Appl. Phys. Lett.* **55**, 1859 (1989).
- <sup>16</sup>B. Vinter and F. Chevoir, in *Resonant Tunneling: Physics and Applications*, (Ref. 8).
- <sup>17</sup>P. Guéret, C. Rossel, E. Marclay, and H. Meier, *J. Appl. Phys.* **66**, 4312 (1989).
- <sup>18</sup>R. Göttinger, A. Gold, G. Abstreiter, G. Weinman, and W. Schlapp, *Europhys. Lett.* **6**, 183 (1988).
- <sup>19</sup>W. R. Frensley, *Solid State Electron.* **32**, 1235 (1989).
- <sup>20</sup>T. Ando, A. B. Fowler, and F. Stern, *Rev. Mod. Phys.* **437** (1982).
- <sup>21</sup>F. Chevoir and B. Vinter (unpublished).